CELL CYCLE
2023, VOL. 22, NO. 6, 693–704
https://doi.org/10.1080/15384101.2022.2145817

Taylor & Francis
Taylor & Francis Group

RESEARCH PAPER

SKA1 is overexpressed in laryngocarcinoma and modulates cell growth via P53 signaling pathway

Zheng Li[a], Jiali Liu[b,#], Haisen Peng[b], Chunhua Li[b], Yuehui Liu[b], and Wen Xie[b]

[a]Department of Radiation and Medical Oncology, Zhongnan Hospital of Wuhan University, Wuhan, China; [b]Department of Otolaryngology, Head and Neck Surgery, The Second Affiliated Hospital of Nanchang University, Nanchang, China

ABSTRACT

Laryngocarcinoma is one of the most frequent malignancies occurring in the head and neck. The roles of spindle- and kinetochore-associated complex 1 (SKA1) in the malignant progression of several cancers have already been discussed. However, the precise significance and action's mechanism of SKA1 in laryngocarcinoma remain largely unknown. In this study, SKA1 was shown to be strongly expressed in laryngocarcinoma tissues and cells, and higher expression of SKA1 was associated with more severe tumor infiltration, larger tumor diameter, higher risk of lymphatic metastasis and later pathological stage. Additionally, loss-of-function assays *in vitro* suggested that SKA1 depletion caused a reduction in cell proliferation, migration, and colony formation as well as an increase in apoptosis. In animal experiments, tumors generated from AMC-HN-8 cells with SKA1 depletion exhibited declined tumor volume and weight. Similarly, the detection of Ki67 protein in xenograft tumor tissues reflected that knocking down SKA1 curbed tumor growth *in vivo*. Further exploration on downstream mechanism revealed that after treatment with Pifithrin-α, the suppression in proliferation level caused by SKA1 knockdown was reversed, while the increase of cell apoptosis was withdrawn; at the molecular level, Pifithrin-α treatment caused p-P53 and Bax diminished, while Bcl-2 ameliorated. In short, SKA1 promotes the development of laryngocarcinoma via activating the P53 signaling pathway.

ARTICLE HISTORY
Received 29 December 2021
Revised 16 September 2022
Accepted 7 November 2022

KEYWORDS
Laryngocarcinoma; SKA1; P53 signaling pathway

Introduction

Laryngocarcinoma is one of the most frequent malignancies occurring in the head and neck [1]. According to the latest update from GLOBOCAN (IARC, WHO), there were an estimated 184,615 new larynx cancer cases and 99,840 larynx cancer deaths worldwide in 2020 [2]. Due to the lack of effective biomarkers for early diagnosis, most patients suffering from laryngocarcinoma are already at an advanced stage when they are diagnosed [3]. Although chemotherapy, radiotherapy, and surgical treatment have made significant progress, the 5-years survival rate of laryngocarcinoma patients is still less than 50% owing to its potentially high morbidity and incommensurably low cure rate [4,5]. Coupled with the adverse side effects of these therapies, it is necessary to explore the underlying mechanism of laryngocarcinoma and identify new therapeutic target so as to improve the clinical prognosis of laryngocarcinoma patients.

Spindle and kinetochore associated complex (SKA complex) is responsible for timely anaphase onset, which included three proteins: SKA1, SKA2, and SKA3. These proteins are engaged in the continuous movement of microspheres and the depolymerization of microtubules. Separately, SKA1 complex mainly performs two key biochemical functions: one is to directly bind to microtubules through its C-terminal domain, and the other is to participate in microtubule-stimulated oligomerization [6,7]. Besides, it has been evidenced that inhibition of the SKA1 complex leads to the loss of chromosomal function, accompanied by cell death [8–11]. On the other hand, the roles of SKA1 in the malignant progression of several cancers have already been discussed recently [12–15]. However,

CONTACT Wen Xie xiongwenping1982@163.com Department of Otolaryngology, Head and Neck Surgery, The Second Affiliated Hospital of Nanchang University, No. 1, Minde Road, Donghu District, Nanchang, Jiangxi 330000, China

[#]These authors contribute equally to this study.

the precise roles of SKA1 in laryngocarcinoma development have not yet been investigated.

In the present study, SKA1 expression levels were detected in laryngocarcinoma tissues and cells. Moreover, we employed lentivirus-mediated short hairpin RNA to knock down SKA1 in laryngocarcinoma cell lines and analyzed the effects of SKA1 depletion on laryngocarcinoma development *in vitro* and *in vivo*. In addition to these, we initially investigated the downstream pathway of SKA1 regulating laryngocarcinoma. Accordingly, we found that SKA1 was upregulated in laryngocarcinoma tissues and cell lines, which was critical to the enhanced proliferative and metastatic phenotypes of laryngocarcinoma as well as tumor growth. We further clarified that SKA1 participates in the progression of laryngocarcinoma by activating the P53 signaling pathway, which might become a potential candidate target for the treatment of this deadly disease.

Materials and methods

Collection of tissues samples

A paraffin-embedded tissue microarray containing 44 cases of laryngocarcinoma and 39 cases of non-tumor samples were provided from Xi'an Alina Biological Technology Co., Ltd. This study was approved by the ethical committees of the Second Affiliated Hospital of Nanchang University Institutional Review Board (IRB: 2020114), and prior written informed consents were obtained from all participants.

Cell lines and cell culture

Here, four human laryngocarcinoma cell lines Hep-2, AMC-HN-8, TU212 and TU686 were purchased from American Type Culture Collection (ATCC) (https://www.atcc.org/). Hep-2 and TU212 were cultured in DMEM +10% FBS. AMC-HN-8 and TU686 were grown in H-DMEM +10% FBS and 1640 + 10% FBS, respectively. All the cells were maintained in a 37°C incubator with 5% CO_2.

Immunohistochemistry (IHC)

Deparaffinized laryngocarcinoma and non-tumor sections were repaired with 1× EDTA (Beyotime Biotechnology Co., Ltd, Shanghai, China), and blocked with 3% H_2O_2 for 5 min. Then, the sections were incubated with SKA1 antibody (1:100, BIOSS, # bs-7846 R), Ki-67 (1:100, Abcam, #ab16667) and secondary antibody (goat anti-rabbit IgG H&L (HRP): 1:400, Abcam) overnight at 4°C. After that, DAB and hematoxylin (Baso Diagnostics Inc., Zhuhai, China) were used to stain. Finally, the slides were sealed with neutral resin (China National Pharmaceutical Group Co., Ltd., Beijing, China) and then the images were captured and analyzed under an optical microscope. Intracellular patterns evaluated were based on protein localization (https://www.proteinatlas.org/). That is, it is determined whether it is positive according to the expression position of the antibody. In addition, all slides were randomly assessed by three independent pathologists. Staining scores were divided into: 1 (1%-24%), 2 (25%-49%), 3 (50%-74%) and 4 (75%-100%). The staining intensity was scored from 0 (no signal color) to 3 (light yellow, brown, and dark brown). IHC results were defined based on staining scores and intensity scores, which specifically include negative (0), positive (1–4), ++ positive (5–8) and +++ positive (9–12). The high and moderate expression parameters were determined by the median of IHC scores of all tissues.

Establishment of stably infected cells

The preparation of lentivirus expressing human SKA1 short hairpin RNA (shSKA1) was performed as follows: RNA interference target sequence (GAGGACTTACTCGTTATGTTA) is designed using SKA1 as template by Shanghai Biosciences Co., Ltd. (Shanghai, China). The control was RNAi scramble sequence (TTCTCCGAACGTGTCACGT). After that, the single-stranded DNA oligo containing interference sequence was synthesized, annealed, and then paired to produce double-stranded DNA. Then, the double-stranded DNA was connected to the BR-V-108 vector and transferred into the prepared TOP 10 E. coli competent cells. The positive recombinants were identified by PCR and sent to sequencing for verification. Finally, the qualified plasmids were used for lentivirus packaging.

AMC-HN-8 and TU212 cells (2×10^5) were infected with lentiviral particles containing shSKA1

or shCtrl (1×10^8 TU/mL) under ENI.S+Polybrene condition. Next, the cells were cultured in their medium for 72 h, and the infection efficiency was evaluated under the microscope according to the green fluorescent protein (GFP) inside the cells. A fluorescence efficiency greater than 80% was considered successful.

RNA extraction, cDNA synthesis, and qRT-PCR

After lentivirus infection, total RNA of AMC-HN-8 and TU212 cells was isolated using TRIzol reagent (Sigma, St Louis, MO, USA) for cDNA synthesis and qRT-PCR. 2.0 μg RNA was reverse transcribed using Promega M-MLV Kit (Promega, Heidelberg, Germany), and quantitative real-time PCR (qRT-PCR) was performed with SYBR Green mastermixs Kit (Vazyme, Nanjing, Jiangsu, China) and applied Biosystems 7500 Sequence Detection system. GAPDH served as an internal normalization control. The relative expression of mRNA was evaluated based on the $2^{-\Delta\Delta Ct}$ method. The primers sequences (5′-3′) were listed as follows: the forward primer of SKA1 is TCCCATTTGCCT CAAGTAACAG, the reverse primer is GGAGGC TTCTTTACGGGTTC; the forward primer of GAPDH is TGACTTCAACAGCGACACCCA, the reverse primer is CACCCTGTTGCTGTAGCC AAA.

Western blot assay

After lentivirus infection or Pifithrin-α treatment, AMC-HN-8 and TU212 cells were collected to extract total protein. The 10% SDS-PAGE was used to segregate proteins and performed the subsequent western blot analysis. Firstly, the PVDF membranes were blocked at room temperature for 1 h by adding TBST solution with 5% skim milk. Then, the membranes were incubated with primary antibodies SKA1 (1:1000, Bioss, #bs-7846 R), P53 (1:3000, Proteintech, #60283-2-Ig), p-P53 (1:2000, Proteintech, 28961-1-AP), Bax (1:2000, Wuhan Sanying, 50599-2-Ig), Bcl-2 (1:2000, Abcam, ab182858) and GAPDH (1:3000, Proteintech, #60004-1-lg) and secondary Antibodies Goat Anti-Rabbit (1:3000, Beyotime, # A0208) and Goat Anti-Mouse (1:3000, Beyotime, # A0216) at room temperature for 2 h. After that, the membranes were washed with TBST solution for three times (10 min/time). Finally, the color rendering was conducted by the immobilon Western Chemiluminescent HRP Substrate kit.

Cell proliferation detection

For celigo cell counting assay, AMC-HN-8 and TU212 cells with shSKA1 and shCtrl were digested and resuspended into the cell suspension. 100 μL/well cell suspension (2000 cells/well) was cultured in a 96-well plate. The cell images were taken by Celigo image cytometer (Nexcelom Bioscience, Lawrence, MA, USA) and a continuous 5-day cell proliferation curve was drawn.

Another method for detecting cell proliferation was the CCK8 assay. After treatment with P53 signaling pathway inhibitor: Pifithrin-α, the cells were treated as described above. On the second day, 10 μL CCK-8 reagent was added into the wells. Finally, the OD value was detected at 24 h and 48 h by the microplate reader at 450 nm.

Colony forming assay

The indicated cells were plated in a 6-well plate (500 cells per well) and cultured for 8 days. The colonies were washed with PBS, fixed with 1 mL 4% paraformaldehyde and stained using 500 μL Giemsa (Dingguo, Shanghai, China). Visible clones were recorded by fluorescence microscope (Olympus, Tokyo, Japan).

Wound healing assay

AMC-HN-8 and TU212 cells with shSKA1 and shCtrl were cultured in a 96-well plate at the density of 5×10^4 cells/well. On the next day, the low-concentration serum medium was supplemented, and a scratch tester was used to align the center of the 96-well plate and gently upward push to form scratches. The cells were then washed with serum-free medium and 0.5% FBS was added. Finally, the cells were cultured in an incubator with 5% CO_2 at 37°C. According to the degree of healing, the plate was scanned at the appropriate time and the migration area was analyzed with Cellomics (Thermo, USA).

Transwell assay

The cell migration was detected with Transwell assays. The indicated cells (5×10^4) in 100 µl medium without FBS were seeded on a fibronectin-coated polycarbonate membrane inserted in a Transwell apparatus (Costar, MA). In the lower chamber, 500 µl medium with 10% FBS was added as a chemoattractant. After the cells were cultured for an appropriate time, the cells adhering to the lower surface were fixed and then stained with 1% crystal violet solution for 1 min and counted under a microscope in three random fields.

Detection of cell apoptosis by fluorescence activated cells sorting (FACS)

After lentivirus infection or P53 Pifithrin-α treatment, AMC-HN-8 and TU212 cells were cultured in a 6-well plate at the volume of 2 mL/well. When the cell confluence reached 85%, the cell suspension was centrifuged at 1,300 rpm and the supernatant was discarded. Then, the cells were washed with D-Hanks (4°C, pH = 7.2 7.4) and stained in the dark by adding 10 µL Annexin V-APC (eBioscience, San Diego, CA, USA). The FACSCalibur (BD Biosciences, San Jose, CA, USA) was exploited to evaluate the cell apoptosis levels.

Human phospho-Kinase array-membrane

Protein expression of 39 phospho-kinases in AMC-HN-8 cells following infection was detected by the Human Phospho-Kinase Array-Membrane. After the cells were lysed, the Handling Array membranes were blocked in 2 mL 1×Wash Buffer II and incubated with cell lysates and 1×Biotin-conjugated Anti-Cytokines overnight at 4°C. Finally, the signals of membranes were tracked by chemiluminescence imaging system.

The construction of nude mouse tumor formation model

The animal experiments were approved by the Ethics committee of the Second Affiliated Hospital of Nanchang University Institutional Review Board (IRB: 2020114). Four-week-old female BALB/c nude mice were purchased from Jiangsu Jicui Yaokang Biotechnology Co., Ltd., and kept them in captivity under the following conditions: 5 mice per cage; temperature, 22-25°C; humidity, 50–60%; 12 h light/dark cycle. Adequate water and food supplies ensured that mice could get them freely. Xenograft models were constructed by subcutaneously injecting shSKA1 or shCtrl AMC-HN-8 cells (1×10^7 cells/each) into the right axilla of nude mouse (10 mice/group). The length and width of the tumor were measured to calculate the tumor volume according to the formula (tumor volume=$\pi/6 \times L \times W \times W$) during 20 days of feeding. After the mice were euthanized, the tumors were removed, weighed, and frozen in liquid nitrogen and stored at −80°C.

Statistical analysis

All assays were independently performed in triplicate. All data were analyzed by using GraphPad Prism 6 (San Diego, CA, USA). The data are presented in the form of the mean ± standard deviation (SD). The Sign test was used to analyze the expression difference of SKA1 in cancer and adjacent tissues. The relationship between SKA1 levels and patients' clinicopathological parameters was investigated by the Mann-Whitney *U*-test and Spearman rank correlation analysis. Statistical differences were evaluated using the unpaired *t*-test and the value of *P* less than 0.05 was considered to be significantly different.

Results

SKA1 is upregulated and associated with clinicopathological parameters of laryngocarcinoma patients

We first analyzed SKA1 expression using a tissue microarray of 44 laryngocarcinoma tissues and 39 adjacent non-tumorous tissues. Overall, 25 of 44 (56.8%) cases showed high SKA1 patterns in tumorous tissues, whereas 37 of 39 (94.9%) cases exhibited low SKA1 levels in non-laryngocarcinoma tissues (Figure 1a and Table 1). Based on these, we evaluated the relationship between SKA1 levels and clinicopathological parameters of patients suffering from laryngocarcinoma. The findings of Mann–-Whitney *U*-test indicated that laryngocarcinoma patients with

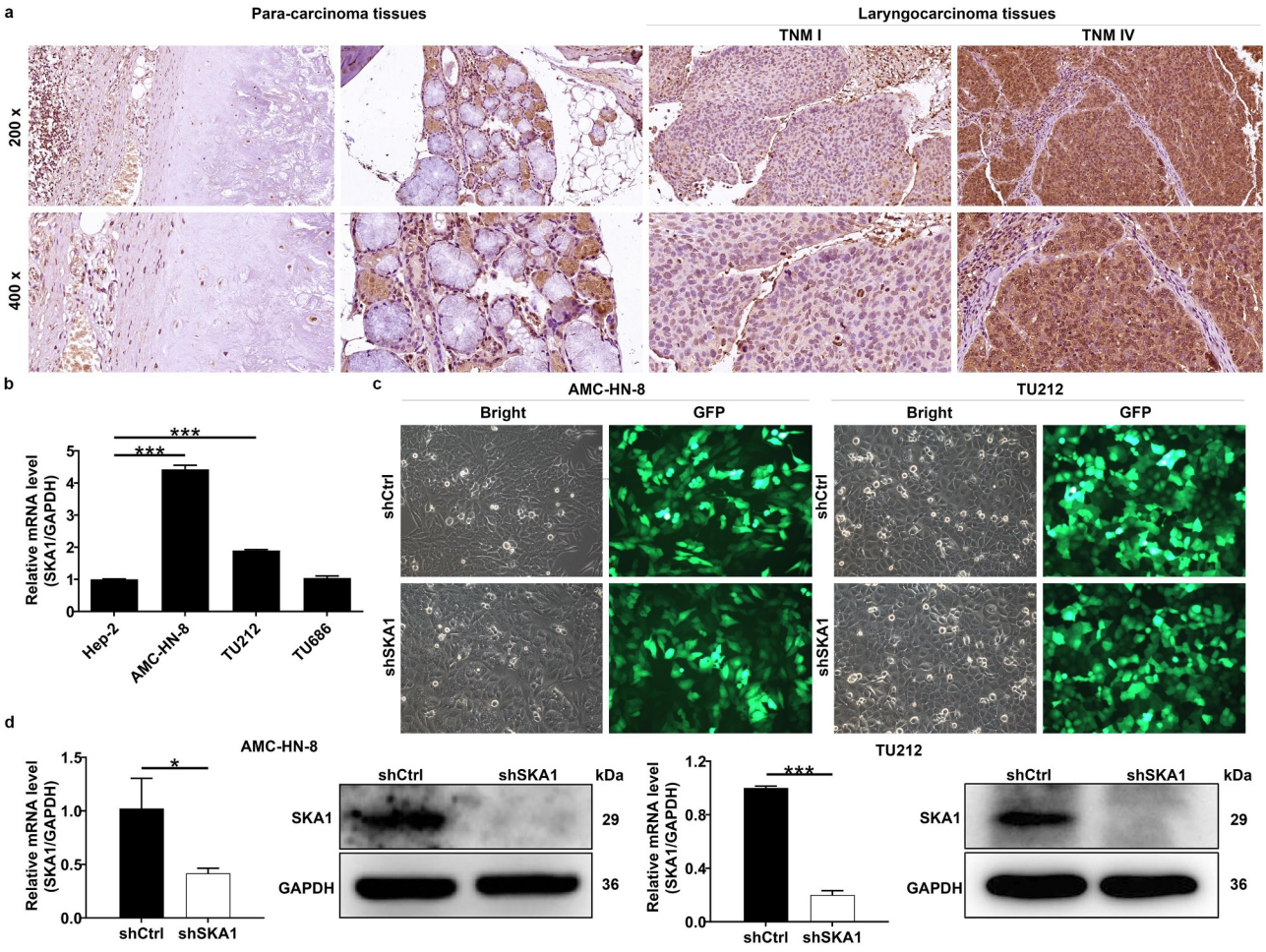

Figure 1. SKA1 was elevated in laryngocarcinoma. (A) The expression of SKA1 in tumor tissues collected from patients diagnosed with laryngocarcinoma was detected by IHC staining and compared with normal tissues. (B) The background expression of SKA1 in laryngocarcinoma cell lines was detected by qRT-PCR. (C) The infection efficiencies of shSKA1 in AMC-HN-8 and TU212 cells were evaluated through observing the fluorescence inside cells. (D) The knockdown efficiencies of SKA1 in AMC-HN-8 and TU212 cells were detected by qRT-PCR and western blotting. *P <0.05, ***P <0.001.

Table 1. Expression patterns of SKA1 in laryngocarcinoma tissues and para-carcinoma tissues revealed in immunohistochemistry analysis.

SKA1 expression	Tumor tissue		Para-carcinoma tissue		P value
	Cases	Percentage	Cases	Percentage	< 0.001
Low	19	43.2%	37	94.9%	
High	25	56.8%	2	5.1%	

abundant SKA1 expression harbored more severe tumor infiltration, larger tumor diameter, higher risk of lymphatic metastasis and later pathological stage than those patients with low levels of SKA1 (Table 2), which was also verified by Spearman rank correlation analysis (Table 3). Moreover, we also found that SKA1 mRNA level was frequently expressed in a panel of laryngocarcinoma cell lines, especially in AMC-HN-8 and TU212 cell lines (Figure 1b). Taken together, these results implied that SKA1 might exert its role as a cancer-promoting factor in laryngocarcinoma development.

SKA1 promotes laryngocarcinoma cell proliferation and migration *in vitro*

To unveil the functional roles of SKA1 in laryngocarcinoma development, we constructed laryngocarcinoma cell lines (AMC-HN-8 and TU212) with stable SKA1 downregulation using a lentiviral shRNA approach. The infection efficiency of

Table 2. Relationship between SKA1 expression and tumor characteristics in patients with laryngocarcinoma.

Features	No. of patients	SKA1 expression		*P* value
		low	high	
All patients	44	19	25	
Age (years)				0.520
< 62	21	8	13	
≥ 62	23	11	12	
Gender				0.383
Male	43	19	24	
Female	1	0	1	
Differentiation				0.677
Low	3	1	2	
Medium	11	6	5	
High	29	12	17	
T				0.008
T1	13	10	3	
T2	19	6	13	
T3	7	2	5	
T4	5	1	4	
N				0.001
N0	32	19	13	
N1	4	0	4	
N2	8	0	8	
Maximum tumor diameter				0.028
≤ 2cm	24	14	10	
> 2cm	20	5	15	
TNM				< 0.001
I	12	10	2	
II	11	6	5	
III	9	2	7	
IV	12	1	11	

Table 3. Relationship between SKA1 levels with laryngocarcinoma patients' clinicopathological parameters.

		SKA1
Maximum tumor diameter	Spearman correlation	0.335
	Signification (double-tailed)	0.026
	N	44
T	Spearman correlation	0.404
	Signification (double-tailed)	0.006
	N	44
N	Spearman correlation	0.528
	Signification (double-tailed)	0.000
	N	44
TNM	Spearman correlation	0.598
	Signification (double-tailed)	< 0.001
	N	44

shSKA1 was assessed by observing the fluorescence signal of the GFP label on the lentivirus used to infect AMC-HN-8 and TU212 cells (Figure 1c). Furthermore, detection of SKA1 mRNA and protein levels by qRT-PCR and western blotting assays illustrated that SKA1 was successfully knocked down in AMC-HN-8 and TU212 cells (Figure 1d). Thus, these both cell lines were employed in subsequent cell function experiments.

Next, celigo cell counting assay was conducted to assess the effects of SKA1 knockdown on cell proliferation. The results demonstrate that silencing SKA1 significantly weakened the proliferative abilities of both cells (Figure 2a). Additionally, the results of colony forming assay performed in AMC-HN-8 and TU212 cells further confirmed that suppression of SKA1 expression attenuated cell viability and proliferation of laryngocarcinoma cells (Figure 2b). Furthermore, we found that cells with depleted SKA1 displayed obviously attenuated capacities of migration (Figure 2c and 2d). More interestingly, flow cytometry experiments demonstrated that SKA1 knockdown markedly promoted cell apoptosis (Figure 2e). Collectively, these *in vitro* results demonstrated that SKA1 knockdown could hamper the development of laryngocarcinoma, as indicated by suppressed proliferation and migration, as well as facilitating apoptosis.

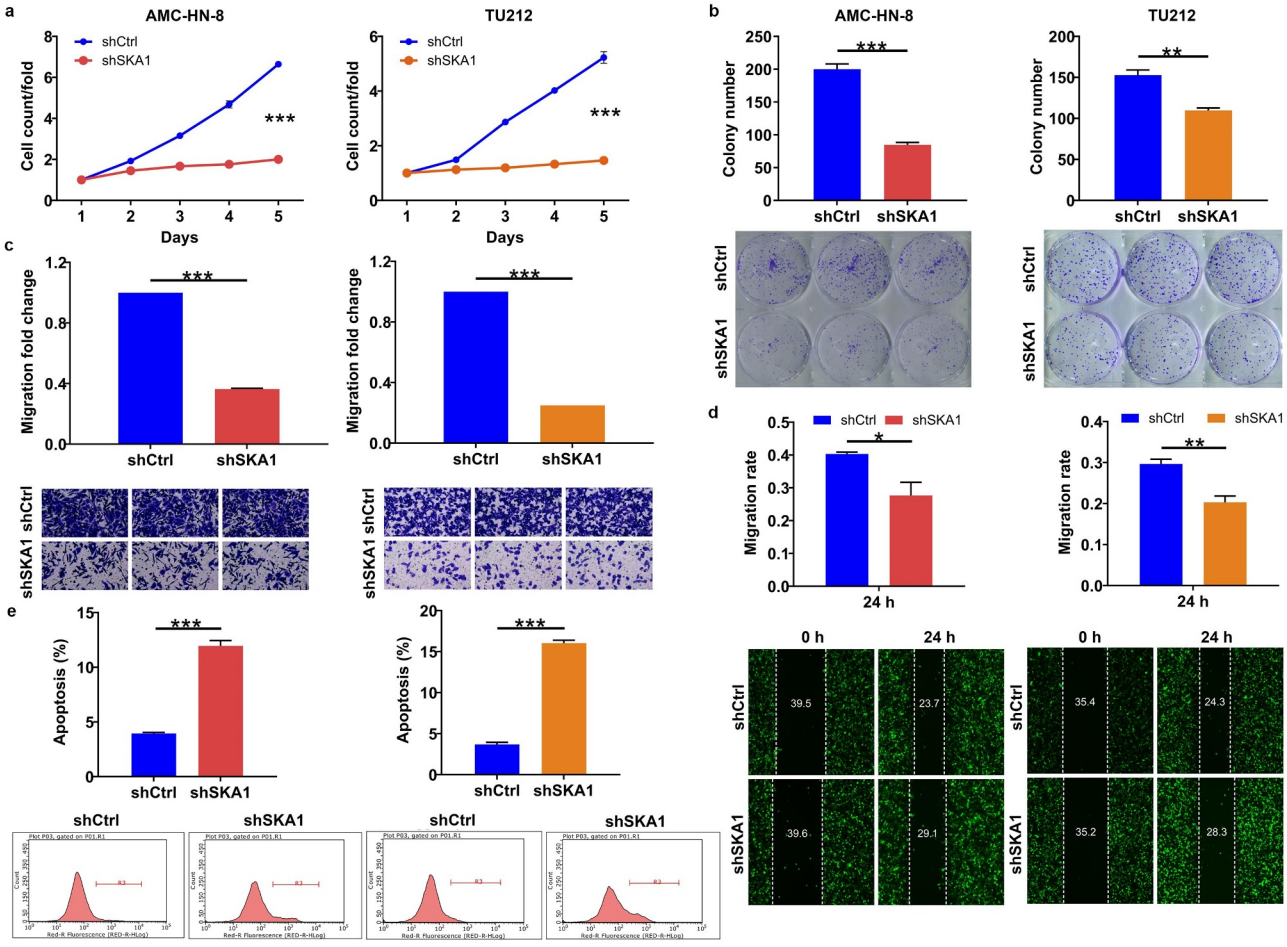

Figure 2. SKA1 knockdown inhibited laryngocarcinoma cell proliferation and cell migration as well as enhanced apoptosis. (A) The Celigo cell counting assay was performed to evaluate cell proliferation of AMC-HN-8 and TU212 cells with or without SKA1 knockdown. (B) The abilities of AMC-HN-8 and TU212 cells to form colonies were assessed upon knocking down SKA1. (C, D) The effects of SKA1 knockdown on cell migration of AMC-HN-8 and TU212 cells were evaluated by transwell assay (C) and wound-healing assay (D). (E) Flow cytometry was utilized to detect cell apoptosis of AMC-HN-8 and TU212 cells upon SKA1 knockdown. *P <0.05, **P <0.01, ***P <0.001.

SKA1 promotes laryngocarcinoma tumor outgrowth *in vivo*

In this section, we aimed to further evidence the previous findings through *in vivo* assays, we examined the effects of SKA1 depletion on tumor formation capacity by using xenograft mouse model. shSKA1 and shCtrl AMC-HN-8 cells were cultured and subcutaneously injected into the right axilla of nude mouse. Twenty days later, the mice were killed, and the tumors were collected for taking photograph and histological analyses. The mouse xenograft experiment demonstrated that SKA1 knockdown showed potent suppression in the formation and growth ability of tumors (Figures 3a–3c). We further assessed the proliferation index (Ki-67) in different groups of tumors by IHC analysis, the results showed significantly lower level of Ki-67 in tumors generated from shSKA1 AMC-HN-8 cells (Figure 3d). Together, these data confirmed that inhibition of SKA1 could significantly delay the growth of xenografted tumors.

P53/bcl-2/bax signaling pathway participates in SKA1-mediated laryngocarcinoma development

Finally, we made a preliminary investigation on the downstream pathway behind SKA1 moderating laryngocarcinoma. We accordingly knocked down SKA1 in AMC-HN-8 cells and analyzed the changes in the levels of 39 phospho (p)-kinases through a Human Phospho-Kinase Array-

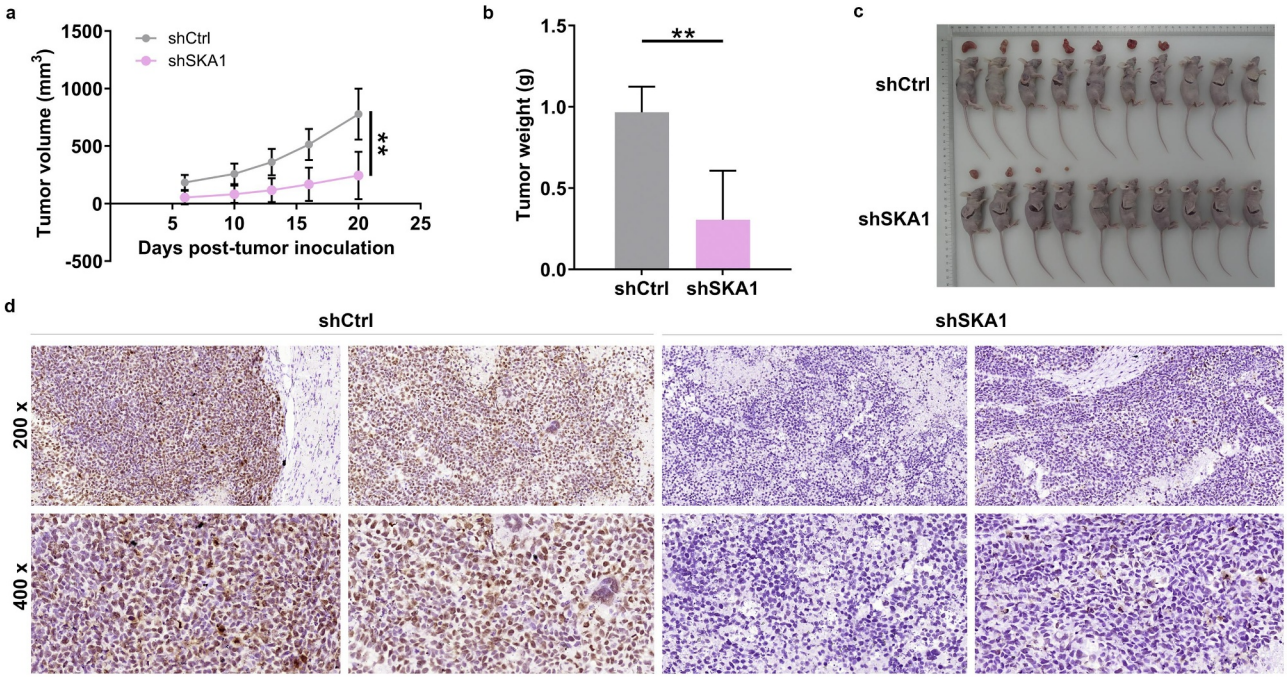

Figure 3. SKA1 knockdown inhibited tumor growth in mice xenograft model. (A) the volume of tumors formed in mice xenograft models was calculated based on the measurement of tumor size. Tumor volume=π/6×L×W×W, where L is tumor length and W is tumor width. (B) the weight of tumors was measured after removing the tumors from the mice. (C) the photos of tumors removed from animal models were obtained after sacrificing the mice. (D) Ki-67 levels were measured through IHC staining in tumor tissues from shCtrl and shSKA1 mice. $^{**}P < 0.01$.

Membrane. Our data demonstrated that SKA1 downregulation increased Akt1/2/3 (S473), Chk-2 (T68), Hsp27 (S78/S82) and p53 (S46), as well as decreased the patterns of multiple p-kinases including GSK-3α/β (S21/S9), GSK-3β (S9), JNK1/2/3 (T183/Y185, T221/Y223), RSK1/2 (S221/S227), STAT2 (Y689), STAT5a/b (Y694/Y699), STAT3 (S727), although the changes of some were slight (Figure 4a and 4b). Notably, it was previously reported that SKA1 could affect the prognosis of lung adenocarcinoma through P53 signaling pathway [16]. More importantly, P53 pathway has been revealed to be involved in laryngocarcinoma development [17,18]. Herein, we speculated that SKA1 probably regulate laryngocarcinoma via activating P53 pathway. To verify this hypothesis, AMC-HN-8 cells with SKA1 downregulation were treated using Pifithrin-α (the inhibitor of P53 signaling pathway). We observed that, after treatment with Pifithrin-α, the suppression in proliferation level caused by SKA1 knockdown was reversed, while the increase of cell apoptosis was withdrawn (Figure 4c and 4d). To further verify these effects at the molecular level, we analyzed the alterations of P53 and its downstream target proteins, such as Bax and Bcl-2 after Pifithrin-α treatment, followed by a restraint in p-P53, Bax, and an augment in Bcl-2 compared with the untreated group (Figure 4e). Thus, we concluded that SKA1 might promote the development of laryngocarcinoma via activating the P53 signaling pathway.

Discussion

Accumulated documents have revealed that SKA1 is a cancer-promoting factor, which is involved in the development of a range of cancer types. For instance, a study from Li *et al.* have reported that upregulation of SKA1 could result in spontaneous tumorigenesis in the transgenic mouse model [19]. Qin *et al.* analyzed the expression of SKA1 in 38 hepatocellular carcinoma cases and found that SKA1 expression was upregulated in hepatocellular carcinoma tissues [14]. Besides, overexpression of SKA1 has been also found in gastric, oral and prostate cancer, and could promote cancer cell proliferation and colony formation in these

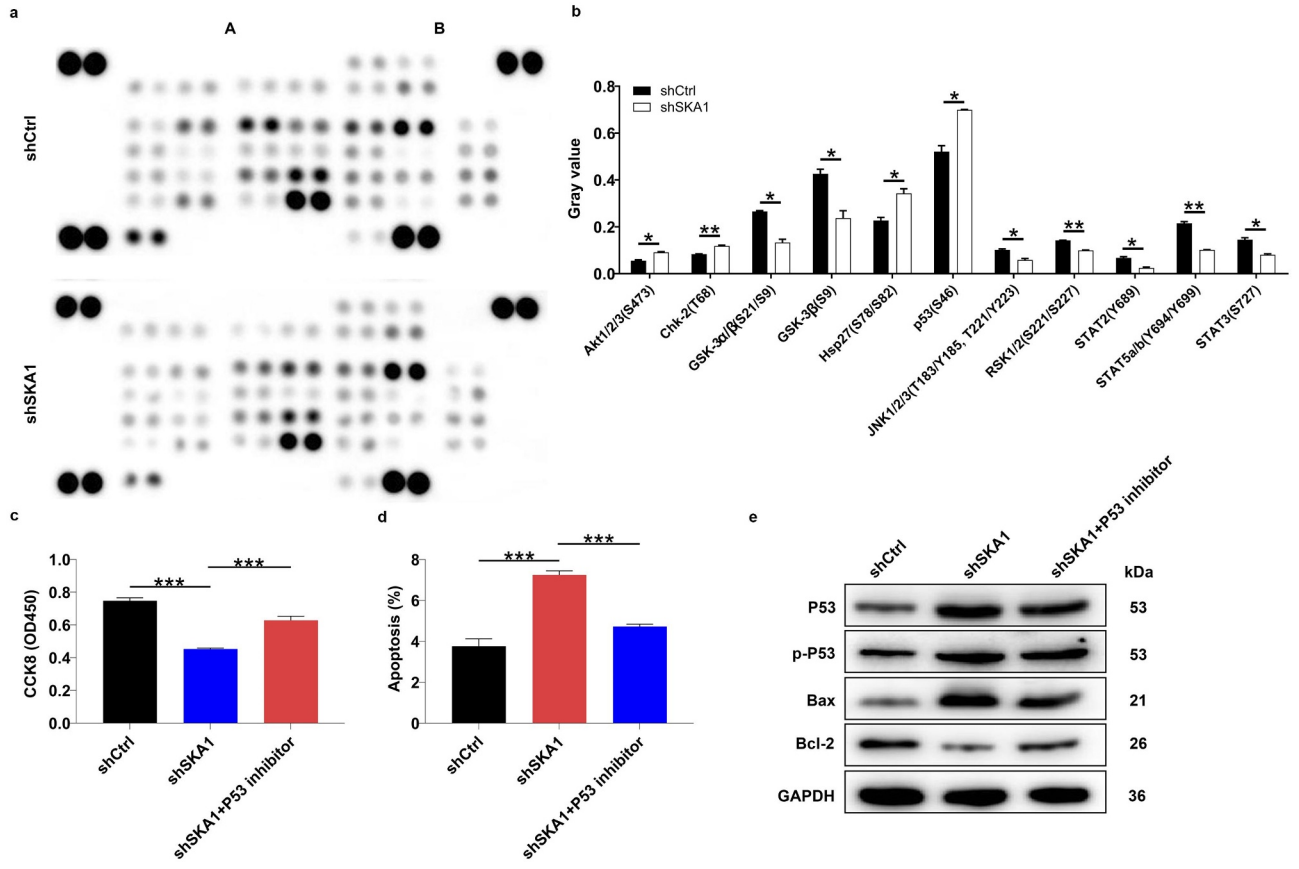

Figure 4. P53/bcl-2/bax signaling pathway participates in SKA1-mediated laryngocarcinoma development. (A, B) Human phospho-kinase array-membrane was used to identify the differential expression of 39 phospho (p)-kinases in AMC-HN-8 cells with SKA1 downregulation. (C, D) After P53 Pifithrin-α treatment, cell proliferation (C) and apoptosis (D) were assessed in AMC-HN-8 cells with SKA1 downregulation. (E) After P53 Pifithrin-α treatment, the levels of P53 and its downstream target proteins Bax and Bcl-2 in AMC-HN-8 cells with SKA1 downregulation were analyzed by western blotting. *P <0.05, **P <0.01, ***P <0.001.

malignancies, while inhibition of SKA1 led to cell cycle arrest and apoptosis [15,20,21]. In consistency with these findings, we found that SKA1 acts as a crucial regulator of malignant phenotypes in laryngocarcinoma progression and confirmed that SKA1 expression increased along with advances of laryngocarcinoma stage, tumor infiltration, and lymphatic metastasis. Based on these findings, we further investigated the biological functions of SKA1 in laryngocarcinoma progression and figured out that it could significantly promote laryngocarcinoma cell proliferation and migration abilities, as well as suppress cell apoptosis. With a xenograft tumor model, we observed that SKA1 could facilitate tumor outgrowth in laryngocarcinoma. However, the detailed mechanisms by which SKA1 exerts these effects remained unclear and thus warrant further investigations.

Although precise regulatory network of SKA1 remains to be elucidated, it has been proposed that SKA1 could affect the prognosis of lung adenocarcinoma through P53 signaling pathway [16]. As we all know, P53 signaling pathways are a fundamental growth control pathway, and its dysregulation frequently occurs in a variety of cancers [22–25]. More interestingly, P53 pathway has been illustrated to be linked to malignant transformation of head and neck precancer, poor head and neck cancer prognosis, as well as head and neck cancer development. In detail, a study from Tandon *et al.* identified that p53 is a prognostic factor of survival in squamous cell carcinoma [26]. Another study from Ramos-García *et al.* indicated that p53 elevation implies the malignant transformation risk of oral potentially malignant disorders [27]. Moreover, Li *et al.* showed that liriodenine induces the apoptosis of human

laryngocarcinoma cells via the upregulation of P53 expression [17]. Gu *et al.* reported that miR-552 promotes laryngocarcinoma cell proliferation and metastasis by targeting P53 pathway [18]. These findings reminded us that SKA1 might exert its roles via P53 pathway in laryngocarcinoma. To verify this hypothesis, we treated AMC-HN-8 cells with depleted SKA1 using Pifithrin-α. As expected, after treatment with Pifithrin-α, the suppression in proliferation level caused by SKA1 knockdown was reversed, while the increase of cell apoptosis was withdrawn. On the other hand, the main way of P53 mediated apoptosis is to promote the gene transcription of downstream pro-apoptotic factors, which in turn triggers mitochondrial pathways [22]. Here, we have to mention the mitochondrial dysfunction mediated by the Bcl-2 family, which is an important event of cell apoptosis [28–30]. In the Bcl-2 family, Bcl-2 and Bax are the representatives of suppressing and enhancing cell apoptosis, respectively. One more thing that needs to be focused is that P53/Bcl-2/Bax interaction has been approved to trigger cell apoptosis in multiple diseases [28,31–33]. Herein, we analyzed the alterations of P53 and its downstream target proteins Bax and Bcl-2 in AMC-HN-8 cells where SKA1 was silenced, suggesting that p-P53 and Bax ameliorated, while Bcl-2 attenuated. Upon Pifithrin-α treatment, these changes were partially abolished. Thus, we concluded that SKA1 might promote the development of laryngocarcinoma via activating the P53/Bcl-2/Bax signaling pathway.

Laryngocarcinoma is a common head and neck malignancy. Although our study proposed that SKA1 participates in the progression of laryngocarcinoma by activating the P53 signaling pathway, the downstream target of SKA1 regulating laryngocarcinoma remains unknown. Many published literature reported that Cyclin D1 plays an important role in the progression of premalignant head and neck lesions to cancer and adjacent epithelium, and it represents a prognostic indicator for head and neck cancer patients, also including laryngeal carcinomas [34–37]. On the other hand, it has been evidenced that knockdown of SKA1 downregulated the expression of Cyclin D1 in human adenoid cystic carcinoma and bladder cancer [38,39]. Thus, we speculated that SKA1 might target Cyclin D1 to participate in the development of laryngeal cancer. Of course, this requires more data to support.

In summary, our study reported the first evidence that SKA1 regulates laryngocarcinoma via the P53 signaling pathway. Thus, we uncovered a novel mechanism of SKA1 in regulating laryngocarcinoma, suggesting that SKA1 may be an attractive therapeutic molecule for treatment of laryngocarcinoma. Although our current research provided some important findings, we have not yet determined the relationship between SKA1 expression and the prognosis of laryngocarcinoma patients. Moreover, histological grade was not also presented in this study. In addition, some statistical analyses performed may be underpowered due to the small sample size. More studies are needed to support the promotion role of SKA1 in laryngocarcinoma.

Disclosure statement

No potential conflict of interest was reported by the authors.

Funding

This study was conducted with support from Science and Technology Department of Jiangxi Province (20202BBGL73017).

Author contributions

Wen Xie designed this research. Zheng Li, Jiali Liu, Chunhua Li and Haisen Peng operated the cell and animal experiments. Zheng Li and Jiali Liu conducted the data procession and analysis. Zheng Li completed the manuscript which was reviewed by Yuehui Liu. All the authors have confirmed the submission of this manuscript.

References

[1] Miller KD, Goding Sauer A, Ortiz AP, et al. Cancer statistics for Hispanics/latinos, 2018. CA Cancer J Clin. 2018 Nov;68(6):425–445.

[2] Sung H, Ferlay J, Siegel RL, et al. Global cancer statistics 2020: gLOBOCAN estimates of incidence and mortality worldwide for 36 cancers in 185 countries. CA Cancer J Clin. 2021 May;71(3):209–249.

[3] Lampri ES, Chondrogiannis G, Ioachim E, et al. Biomarkers of head and neck cancer, tools or a Gordian knot? Int J Clin Exp Med. 2015;8 (7):10340–10357.
[4] Morshed K. Association between human papillomavirus infection and laryngeal squamous cell carcinoma. J Med Virol. 2010 May;82(6):1017–1023.
[5] Zhuo XL, Wang Y, Zhuo WL, et al. Possible association of Helicobacter pylori infection with laryngeal cancer risk: an evidence-based meta-analysis. Arch Med Res. 2008 Aug;39(6):625–628.
[6] Welburn JP, Grishchuk EL, Backer CB, et al. The human kinetochore Ska1 complex facilitates microtubule depolymerization-coupled motility. Dev Cell. 2009 Mar;16(3):374–385.
[7] Abad MA, Medina B, Santamaria A, et al. Structural basis for microtubule recognition by the human kinetochore Ska complex. Nat Commun. 2014;5:2964.
[8] Hanisch A, Sillje HH, Nigg EA. Timely anaphase onset requires a novel spindle and kinetochore complex comprising Ska1 and Ska2. EMBO J. 2006 Nov 29;25 (23):5504–5515. DOI:10.1038/sj.emboj.7601426
[9] Rice L, Waters CE, Eccles J, et al. Identification and functional analysis of SKA2 interaction with the glucocorticoid receptor. J Endocrinol. 2008 Sep;198 (3):499–509.
[10] Chan YW, Jeyaprakash AA, Nigg EA, et al. Aurora B controls kinetochore-microtubule attachments by inhibiting Ska complex-KMN network interaction. J Cell Biol. 2012 Mar 5;196(5):563–571. DOI:10.1083/jcb.201109001
[11] Jeyaprakash AA, Santamaria A, Jayachandran U, et al. Structural and functional organization of the Ska complex, a key component of the kinetochore-microtubule interface. Mol Cell. 2012 May 11;46(3):274–286. DOI:10.1016/j.molcel.2012.03.005
[12] Arai T, Okato A, Kojima S, et al. Regulation of spindle and kinetochore-associated protein 1 by antitumor miR-10a-5p in renal cell carcinoma. Cancer Sci. 2017 Oct;108(10):2088–2101.
[13] Dong C, Wang XL, Ma BL. Expression of spindle and kinetochore-associated protein 1 is associated with poor prognosis in papillary thyroid carcinoma. Dis Markers. 2015;2015:616541.
[14] Qin X, Yuan B, Xu X, et al. Effects of short interfering RNA-mediated gene silencing of SKA1 on proliferation of hepatocellular carcinoma cells. Scand J Gastroenterol. 2013 Nov;48(11):1324–1332.
[15] Sun W, Yao L, Jiang B, et al. Spindle and kinetochore-associated protein 1 is overexpressed in gastric cancer and modulates cell growth. Mol Cell Biochem. 2014 Jun;391(1–2):167–174.
[16] Chen C, Guo Q, Song Y, et al. SKA1/2/3 serves as a biomarker for poor prognosis in human lung adenocarcinoma. Transl Lung Cancer Res. 2020 Apr;9 (2):218–231.
[17] Li L, Xu Y, Wang B. Liriodenine induces the apoptosis of human laryngocarcinoma cells via the upregulation of p53 expression. Oncol Lett. 2015 Mar;9(3):1121–1127.
[18] Gu J, Han T, Sun L, et al. miR-552 promotes laryngocarcinoma cells proliferation and metastasis by targeting p53 pathway. Cell Cycle. 2020 May;19 (9):1012–1021.
[19] Li J, Xuan JW, Khatamianfar V, et al. SKA1 over-expression promotes centriole over-duplication, centrosome amplification and prostate tumourigenesis. J Pathol. 2014 Oct;234(2):178–189.
[20] Zhang B, Li KY, Chen HY, et al. Spindle and kinetochore associated complex subunit 1 regulates the proliferation of oral adenosquamous carcinoma CAL-27 cells in vitro. Cancer Cell Int. 2013 Aug 20;13(1):83. DOI:10.1186/1475-2867-13-83
[21] Wang K, Sun J, Teng J, et al. Overexpression of spindle and kinetochore-associated protein 1 contributes to the progression of prostate cancer. Tumour Biol. 2017 Jun;39(6):1010428317701918.
[22] Pei L, Shang Y, Jin H, et al. DAPK1-p53 interaction converges necrotic and apoptotic pathways of ischemic neuronal death. J Neurosci. 2014 May 7;34(19):6546–6556. DOI:10.1523/JNEUROSCI.5119-13.2014
[23] Sherr CJ, McCormick F. The RB and p53 pathways in cancer. Cancer Cell. 2002 Aug;2(2):103–112.
[24] Wei GH, Wang X. lncRNA MEG3 inhibit proliferation and metastasis of gastric cancer via p53 signaling pathway. Eur Rev Med Pharmacol Sci. 2017 Oct;21 (17):3850–3856.
[25] Jin CY, Du L, Nuerlan AH, et al. High expression of RRM2 as an independent predictive factor of poor prognosis in patients with lung adenocarcinoma. Aging (Albany NY). 2020 Dec 19;13(3):3518–3535. DOI:10.18632/aging.202292
[26] Tandon S, Tudur-Smith C, Riley RD, et al. A systematic review of p53 as a prognostic factor of survival in squamous cell carcinoma of the four main anatomical subsites of the head and neck. Cancer Epidemiol Biomarkers Prev. 2010 Feb;19(2):574–587.
[27] Ramos-Garcia P, Gonzalez-Moles MA, Warnakulasuriya S. Significance of p53 overexpression in the prediction of the malignant transformation risk of oral potentially malignant disorders: a systematic review and meta-analysis. Oral Oncol. 2022 Mar;126:105734.
[28] Beberok A, Wrzesniok D, Rok J, et al. Ciprofloxacin triggers the apoptosis of human triple-negative breast cancer MDA-MB-231 cells via the p53/bax/bcl-2 signaling pathway. Int J Oncol. 2018 May;52(5):1727–1737.
[29] Tsujimoto Y. Role of Bcl-2 family proteins in apoptosis: apoptosomes or mitochondria? Genes Cells. 1998 Nov;3(11):697–707.
[30] Adams JM, Cory S. The Bcl-2 protein family: arbiters of cell survival. Science. 1998 Aug 28;281 (5381):1322–1326. DOI:10.1126/science.281.5381.1322

[31] Duan P, Hu C, Butler HJ, et al. 4-Nonylphenol induces disruption of spermatogenesis associated with oxidative stress-related apoptosis by targeting p53-Bcl-2/bax-Fas /FasL signaling. Environ Toxicol. 2017 Mar;32(3):739–753.
[32] Qi B, Cao L, Wang L, et al. Study on apoptosis and expression of P53, bcl-2, Bax in cardiac myocytys of congestive heart failure induced by ventricular pacing. J Tongji Med Univ. 2001;21(3):202–205. DOI:10.1007/BF02886429
[33] Selim AG, El-Ayat G, Wells CA. Expression of c-erbB2, p53, Bcl-2, Bax, c-myc and Ki-67 in apocrine metaplasia and apocrine change within sclerosing adenosis of the breast. Virchows Arch. 2002 Nov;441(5):449–455.
[34] Ramos-Garcia P, Gonzalez-Moles MA, Ayen A, et al. Asymmetrical proliferative pattern loss linked to cyclin D1 overexpression in adjacent non-tumour epithelium in oral squamous cell carcinoma. Arch Oral Biol. 2019 Jan;97:12–17.
[35] Ramos-Garcia P, Gonzalez-Moles MA, Ayen A, et al. Predictive value of CCND1/cyclin D1 alterations in the malignant transformation of potentially malignant head and neck disorders: systematic review and meta-analysis. Head Neck. 2019 Sep;41(9):3395–3407.
[36] Ramos-Garcia P, Gonzalez-Moles MA, Gonzalez-Ruiz L, et al. Clinicopathological significance of tumor cyclin D1 expression in oral cancer. Arch Oral Biol. 2019 Mar;99:177–182.
[37] Gioacchini FM, Alicandri-Ciufelli M, Kaleci S, et al. The prognostic value of cyclin D1 expression in head and neck squamous cell carcinoma. Eur Arch Otorhinolaryngol. 2016 Apr;273(4):801–809.
[38] Tian F, Xing X, Xu F, et al. Downregulation of SKA1 gene expression inhibits cell growth in human bladder cancer. Cancer Biother Radiopharm. 2015 Sep;30 (7):271–277.
[39] Zhao LJ, Yang HL, Li KY, et al. Knockdown of SKA1 gene inhibits cell proliferation and metastasis in human adenoid cystic carcinoma. Biomed Pharmacother. 2017 Jun;90:8–14.